PERGAMON

Engineering Fracture Mechanics 69 (2002) 1391–1399

Engineering Fracture Mechanics

www.elsevier.com/locate/engfracmech

Technical Note

Determination of impact fracture toughness of polyethylene using arc-shaped specimens

J. Niglia, A. Cisilino, R. Seltzer, P. Frontini *

Institute of Materials Science and Technology—INTEMA, Universidad Nacional de Mar del Plata, J.B. Justo 4302, B7608 FDQ, Mar del Plata, Argentina

Received 11 April 2001; received in revised form 21 December 2001; accepted 3 January 2002

Abstract

This paper describes a methodology for the determination of the impact radial fracture toughness, G_{IC}, of cylindrical polymeric molded parts using arc-shaped specimens. The proposed methodology is an extension of the ISO/DIS 17281 Standard which states that for brittle behavior, a basically linear relationship exits between the fracture energy, U; and the energy calibration factor, ϕ. This relationship allows calculating the critical strain energy release rate from the slope of the U vs. ϕ plot. An expression for the energy calibration factor, ϕ, for the arc-shaped specimen is proposed in this work, by combining tabulated functions and finite element results. The methodology is applied to test high density polyethylene arc-shaped specimens taken from cylinder walls. © 2002 Published by Elsevier Science Ltd.

Keywords: Arc-shaped specimens; Energy calibration factor; High density polyethylene; G_{IC} methodology; Impact fracture toughness

1. Introduction

The growing use of polymeric materials in engineering applications demands new methodologies in order to assess the material capability to withstand loads. Impact testing is widely used to characterize the fracture resistance of materials because it attempts to simulate the most severe load conditions to which a material can be subjected. It is well known that thermoplastics, even toughened grades, are relatively susceptible to impact fracture.

Instrumented impact testing is gaining considerable practical importance, as it allows assessing the material toughness under the most critical conditions, given by high strain rates and the presence of notches. The use of fracture mechanics to analyze such tests has greatly improved their utility and, with the recent availability of good high speed recording equipment, there has been much progress reported.

Analysis of the impact toughness of injection and/or extrusion molded semicrystalline polymers, such as polyethylene, presents an additional challenge, due to the interaction between orientation and crystallization leading to a complex, fabrication dependent, anisotropic morphology. This microstructure determines, to a large extent, the fracture and the ultimate properties of the molded part. Understanding the

* Corresponding author. Fax: +54-223-816600.
E-mail address: pmfronti@fi.mdp.edu.ar (P. Frontini).

0013-7944/02/$ - see front matter © 2002 Published by Elsevier Science Ltd.
PII: S0013-7944(02)00008-5

complex relationship between impact resistance, processing, and/or molecular parameters requires that careful attention be directed to the impact measurement itself [1,2].

More specifically, the impact fracture toughness of cylindrical structural pieces like pressure vessels [3], thread protectors [4] and pressurized pipelines for fuel gas and water distribution materials [5–9] can be very important from a practical point of view. As explained above, since processing can significantly influence the final performance, material testing should be made on samples having the same processing history. In this sense, testing for the determination of the material radial fracture toughness may be sometimes rather difficult, since it is not always possible to obtain standard specimens from cylindrical samples. On this purpose, arc-shaped bending specimens may be very useful [8,10–12].

It is the objective of this paper to present an extension to the ISO/DIS 17281 Standard methodology [13,14] for the determination of material radial toughness using arc-shaped specimens. The proposed methodology is employed to test the toughness of high density polyethylene (HDPE) injection molded cylinders.

2. Fracture toughness method

For metals, the elastic modulus E varies very little with strain rate, so the fracture toughness G or K can be found by any path [14]. On the other hand, path is important in the case of polymers as E does vary with rate for these materials. In particular, variation of flexural modulus of polyethylene is both strain and strain-rate dependent [15]. A widely accepted method to determine the high rate fracture toughness (around $1\ \mathrm{m\,s^{-1}}$) for linear-elastic polymeric materials behavior is the G_{IC} methodology [13,16–18]. This quasi-static energy measuring method is less prone to dynamic error and works well for brittle materials, where initiation is followed by instability [17]. Previous work showed that for brittle behavior a linear relationship exists between the impact fracture energy, U, and the specimen dimension compliance function, $BW\phi$, where B and W are the specimen depth and width respectively, and ϕ is a known function of crack length [19]. The slope of this relationship defines the critical strain energy release rate, G_{IC} [13,16–18]. The kinetic energy of the moving testing specimen and the energy associated with the inertial loads constitute parasitic energy terms [18]. However, as they were demonstrated to be essentially independent of crack length the multi-specimen procedure circumvents the need of evaluating those two terms [16].

At speeds around $1\ \mathrm{m\,s^{-1}}$ the dynamic effects are considered negligible and static equation are still valid [13]. Thus, for a specimen of constant thickness B under elastic conditions, the critical energy release rate at crack growth initiation, G_C, may be determined from the measured load, P, energy, U, or displacement, δ, from the relationships [17,18]

$$G = \frac{P^2}{2B}\frac{\mathrm{d}C}{\mathrm{d}a} \tag{1}$$

$$G = \frac{1}{B}\frac{\mathrm{d}U}{\mathrm{d}a} \tag{2}$$

$$U = \tfrac{1}{2}\delta P = \tfrac{1}{2}P^2 C \tag{3}$$

where a is the crack length, and $C(a)$ the compliance of the cracked specimen. In terms of fracture toughness:

$$K^2 = Y^2\sigma^2 a \tag{4}$$

where σ is the maximum gross stress, and Y is a function of the crack length to specimen width W. Since K_C and G_C are related by the well known expression

$$K_C^2 = EG_C \tag{5}$$

(where the Young modulus E is replaced by $E/(1-\nu^2)$ for plane strain), there will exist for any given geometry a constant relationship between gross stress and load σ/P, say α/BW. So that, from Eqs. (1), (4), and (5) we can write

$$\frac{dC}{d(a/W)} = \frac{2\alpha^2}{BE} Y^2(a/W) \tag{6}$$

At the same time, and now in terms of energy, from Eqs. (1) and (3) we can also write

$$G_C = \frac{U}{CBW} \frac{dC}{d(a/W)} \tag{7}$$

or the more usual expression [19]:

$$U = G_C BW\phi \tag{8}$$

where

$$\phi = \frac{C}{dC/d(a/W)} \tag{9}$$

Note that the shape factor ϕ allows calculating G_C by plotting U vs. $BW\phi$. The shape factor ϕ is available in the literature for the most common geometries used in standard impact characterization, the Charpy and Izod specimens [18]. In order to determine ϕ for a specimen other than the Charpy or Izod, Eq. (9) can be employed once the specimen compliance C is known. In this sense an expression for C can be deduced from Y^2 by using Eq. (6);

$$C = \frac{2\alpha^2}{EB} \int Y^2(a/w)\, d(a/w) + C_0 \tag{10}$$

where C_0 is an integration constant.

3. Specimen geometry and ϕ calibration

For the sake of simplicity, studies were performed in this work on standard arc-shaped specimens designed according to ASTM E399-90 [20]. The specimen geometry is sketched in Fig. 1a. The specimen thickness, B, and the span to depth ratio, S/W, were always kept equal to $W/2$ and 4 respectively.

From the K expression reported in literature [20] for arc-shaped specimen the function Y was obtained to yield

$$Y = \frac{2}{3}\left(\frac{a}{W}\right)^{-1/2} [1 + (1 - r_1/r_2)h_1(a/W)] f_1(a/W)$$

$$f_1(a/W) = \frac{0.677 + 1.078(a/W) - 1.43(a/W)^2 + 0.669(a/W)^3}{(1 - a/W)^{3/2}}$$

$$h_1(a/W) = 0.29 - 0.66(a/W)(a/W) + 0.37(a/W)^2 \tag{11}$$

which is considered to be accurate to within $\pm 1\%$ for $0.2 < a/W < 1$. The geometric constant α was taken as for the SE(B) specimen [18]:

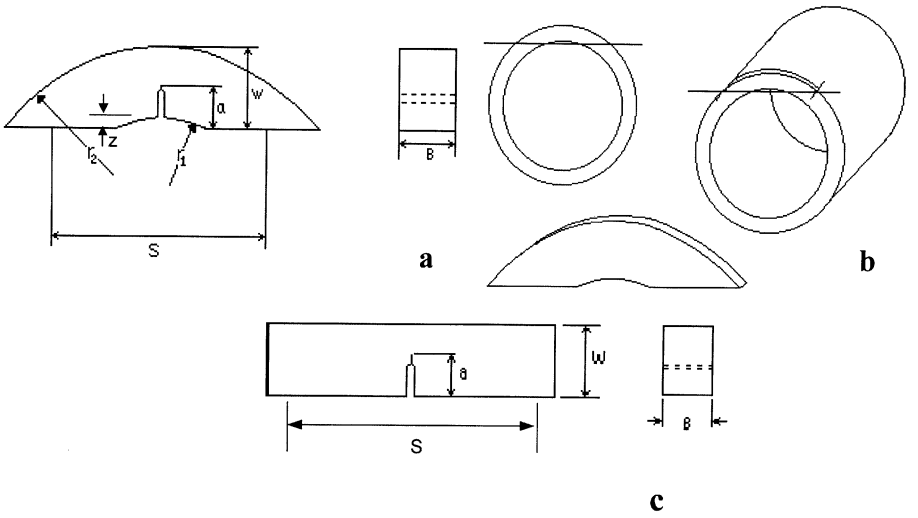

Fig. 1. (a) Standard proportions for the arc-shaped specimen. (b) Arc-shaped bending sample cut from cylinder wall. (c) Standard proportions for the parallelepiped specimen.

$$\alpha = \frac{3}{2}\frac{S}{W} \tag{12}$$

Then, an expression for the compliance can be obtained from Eq. (10), with Y and α, given by (11) and (12) respectively. The integral in (10) was carried out symbolically using MathCad [21]. The resulting expression was simplified by eliminating the least significant terms yielding

$$C' = \left(-52.488 + 10.08r + 1.031r^2\right)x + (2.822 - 10.656r)x^2 + 6.008rx^3 + \left(-14.832 + 11.88r\right)x^4 + \left(-64.224 + 26.064r - 0.202r^2\right)\ln(1-x) - \frac{(19.44 - 5.059r)}{(1-x)} + \frac{(15.84)}{(1-x)^2} \tag{13}$$

where for the sake of simplicity $x = a/W$ and $r = r_1/r_2$. It is worth to note that expression (13) has a deviation of at most 1% with respect to the complete solution.

The term C_0 in Eq. (10) was determined using finite element (FEM) results. It is worth to note that although the ratios B/W, S/W and Z/W are fixed, C_0 is not constant as for the Charpy and Izod specimens, but a function of r_1/r_2. Thus, series of two-dimensional plane-stress FEM models were analyzed using LUSAS [22], in order to determine the functionality of C_0 with r_1/r_2 for the range $0.6 < r_1/r_2 < 1$ (see [20]) and $a/W = 0.20$ (note that from the definition of Y, expression (13) is only considered to be valid $0.2 < a/W < 1$). FEM analyses were performed on unitary thickness models for which the elastic modulus E was set to unity, and $\nu = 0.3$. Model discretizations were constructed using six-node triangular elements without any local mesh refinement. A sample model is shown in Fig. 2, where only one half of the problem was considered by imposing the appropriate boundary conditions.

Obtained results are summarized in Fig. 3. Each of the data points is the product of a quadratic least-square extrapolation to null element size of the results of four FEM models designed to accommodate from 10 to 50 elements along the specimen depth, W. Standard errors of the extrapolated values do not exceed 2%. Finally, data points were interpolated using an exponential decay function to yield:

$$C_{0.2}BE = 15.25 + 3.14\,\mathrm{e}^{\left(0.6-\frac{r_1}{r_2}\right)/0.226} \tag{14}$$

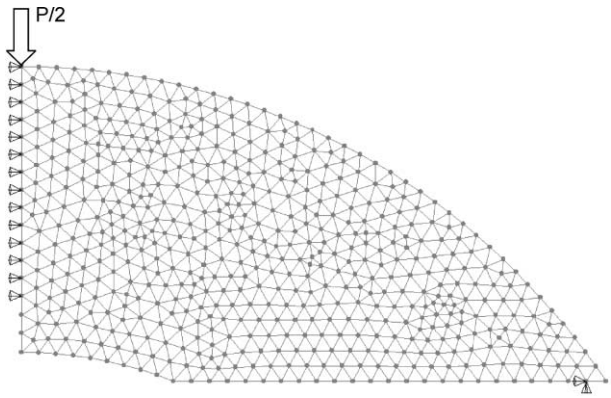

Fig. 2. Sample mesh used in FEM modeling (coarsest mesh for $r_1/r_2 = 0.6$).

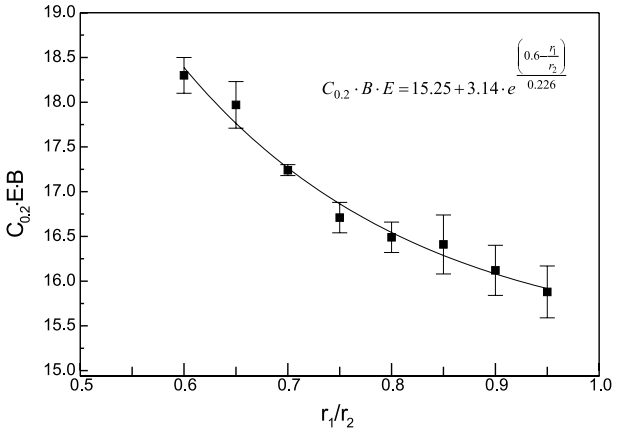

Fig. 3. Normalized compliance for $a/w = 0.2$ as function of internal to external radio ratio. Bars indicate standard error for the extrapolated FEM results.

Eq. (14) fits data points with a maximum error of 1%. The expression for C_0 was obtained from Eq. (10) after replacing (13) and (14) to yield

$$C_0(r) = 10.879 + 3.136\,\mathrm{e}^{(2.655-4.425r)} - 2.165r - 2.51r^2 \tag{15}$$

Finally, a function for ϕ was obtained, in the spirit of the one proposed in [13] for the SE(B) specimen

$$\phi = \frac{C' + C_0}{\mathrm{d}C'/\mathrm{d}x} \tag{16}$$

where

$$\frac{\mathrm{d}C'}{\mathrm{d}x} = -52.488 + 10.080r + 1.031r^2 + (5.645 - 21.312r)x + 18.023rx^2 + (59.328 - 47.52r)x^3 + \frac{(64.224 - 26.064r + 0.202r^2)}{(1-x)} - \frac{(19.44 - 5.059r)}{(1-x)^2} + \frac{31.68}{(1-x)^3} \tag{17}$$

Fig. 4 shows the resulting ϕ vs. a/w data, for different r_1/r_2 ratios. Data for the SE(B) specimen is also included as a reference.

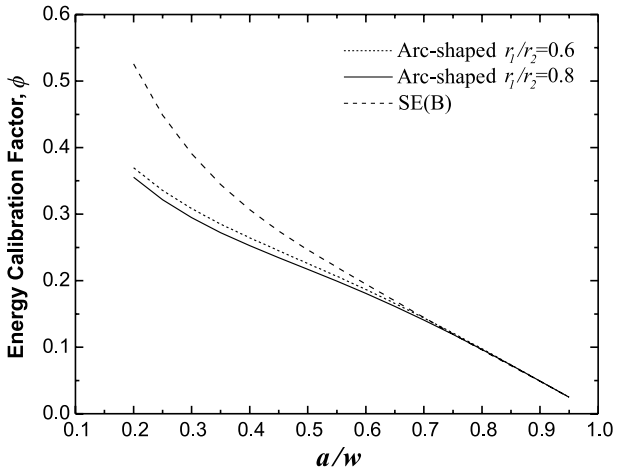

Fig. 4. Energy calibration factor for the arc-shaped specimen as a function of crack length for different r_1/r_2 ratios. Data for the SE(B) specimen is also included as a reference.

4. Experiments

Fracture tests were performed at 1 m s^{-1} using an instrumented falling weight Fractovis 6789 by CEAST in three-point bending configuration (mode I). Two kinds of specimens were used: parallelepipeds and arc-shaped (Fig. 1). Parallelepipeds were machined from sections cut from a molded plate. The original plate was made by compression molding of a commercial injection grade HDPE (see Table 1). Final dimensions of the sample were width, $W = 10$ mm, span, $S = 4W$ and thickness, $B = 2W$. On the other hand, arc-shaped specimens were machined from sections cut from cylinders in the radial orientation (C–R), as sketched in Fig. 1b [20]. The original cylinder was made by injection molding, and using the same HDPE than for the molded plate. The cylinder dimensions, were $r_1 = 110.35$ mm and $r_2 = 124.00$ mm. The sample width, W, was that given by the cylinder thickness.

Sharp notches were introduced at mid span by alternatively sliding a sharp blade scalpel-wise across the samples with a crack to depth ratio (a/W) varying between 0.3 and 0.7. All tests were carried out at room temperature. The spurious contributions to the measured energy due to machine compliance and specimen indentation were corrected following usual practices [16,18].

Fig. 5 is a picture of the fracture surfaces with the corresponding initial notch at the bottom. It is possible to observe a craze zone, which grew from the initial notch and remained almost of constant size (0.5 mm).

Table 1
High-density polyethylene properties

Property (units)	Value
Mass density (kg m^{-3})	948
Young's modulus (MPa)	850
Yield stress (MPa)	25
Melting point (°C)	135
Measured MFR (g per 10 min)[a]	4
Colour	Natural

[a] ASTM D 1238 at 190 °C and 2.16 kg load.

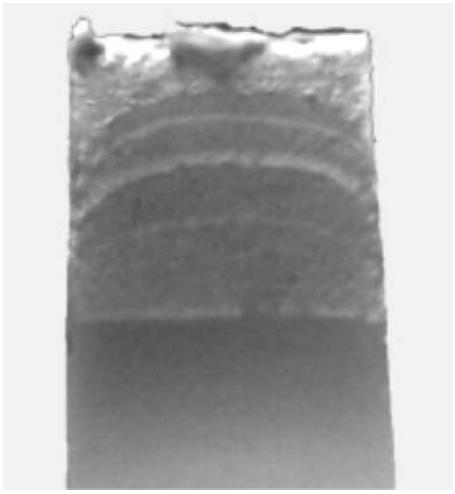

Fig. 5. Fracture surface of the broken sample.

This plastic zone can be considered restricted to a small region near crack tip and hence LEFM is applicable. At the same time, it is possible to observe the arrest marks, which show only a slight curvature indicating that a plane strain conditions prevailed.

Fig. 6 shows the load/time traces. The amplitude of load oscillations are confined to the allowed limits for polymer impact testing, thus enabling the recorded load trace to be used to determine fracture toughness, G_{IC}, as the slope of the average line determined by plotting the total fracture energy as a function of $BW\phi$ [15–17,23].

The shape of the curves was influenced by crack length. Note that as the notch size increased the load rolls over a maximum and starts to fall before showing the abrupt drop, which corresponds to crack initiation. In this paper, we did not take into account for this post-peak ductility, dealing with the initiation event alone. The initiation G_{IC} was determined from the energy to peak load, U_p [15].

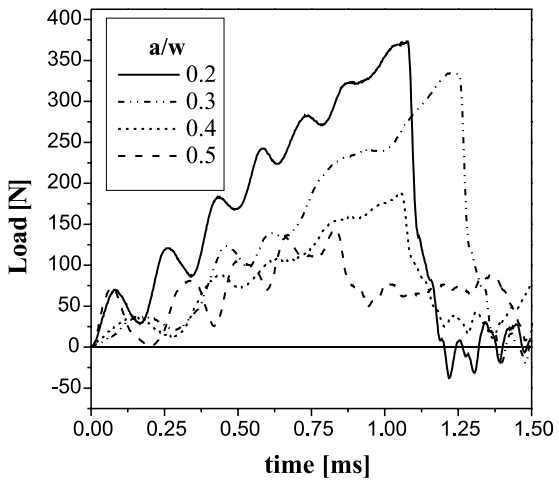

Fig. 6. Obtained load/time traces for the arc-shaped specimens.

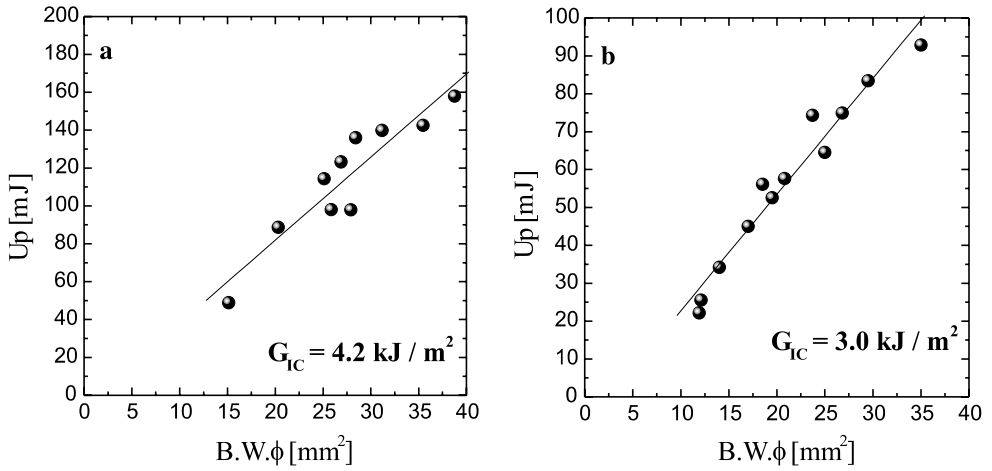

Fig. 7. Corrected impact energy vs. compliance function: (a) arc-shaped specimens and (b) standard SE(B) specimens.

In order to verify the efficacy of the proposed methodology, a set of standard three-point bending specimens [16] prepared from compression-molded plates of the same HDPE material was also tested. Plots of corrected energy vs. $BW\phi$ are shown in Fig. 7 for both, the arc-shaped and standard specimens, showing the expected cyclical variation or bouncing in U for dynamic analysis [24]. The selected $BW\phi$ range allowed to obtained a good average line as proposed by the ISO/DIS 17281 Standard. The predicted, G_{IC}, from the slopes of the plots are consistent with data calculated using standard bending specimens of the same material. Differences in the critical parameters are due to the influence of orientation in the injected pieces. The latter effect may be even more important in the case of extruded pipes for which the application of the proposed methodology appears very promising.

5. Conclusions

This paper describes a methodology for the determination of the impact radial fracture toughness, G_{IC}, of cylindrical polymeric parts using arc-shaped specimens. As the ISO/DIS 17281 Standard, the proposed methodology is based on the fact that for brittle behavior, a linear relationship exists between the fracture energy and the specimen compliance function.

An expression for the energy calibration factor, ϕ, for the arc-shaped specimen was developed by combining tabulated functions and FEM results. The proposed function follows the general shape of the one given by the ISO/DIS 17281 Standard for the SE(B) specimen.

The methodology was applied to test the radial toughness under impact of HDPE molded cylinders. Calibration factors were found close to those of the SE(B) specimen and led to reliable fracture toughness values.

The application of the proposed methodology appears very promising for the determination of the fracture properties extruded pipes due to their inherent anisotropic morphology.

References

[1] Dormier EJ, Yamoska BS, Dan E. Evaluation of linear polyethylene by instrumented impact analysis. Proceedings of ANTEC'84, 1984. p. 294–296.

[2] Lu X, Zhou Z, Brown N. The anisotropy of slow crack growth in polyethylene pipes. Polym Eng Sci 1994;34:109–15.
[3] Mouzakis DE, Karger-Kocsis J. Effects of gasoline absorption on the tensile impact response of HDPE/Selar™ laminar microlayer composites. J Appl Polym Sci 1998;68:561–9.
[4] Dale BA, Moyer MC, Sampson TW. A test program for the evaluation of oil filed thread protectors. J Pet Technol 1985:306–14.
[5] Wheel MA, Leevers PS. High speed double torsion tests on tough polymers. II: nonlinear elastic dynamic analysis. Int J Fract 1993;61:349–59.
[6] Greig JM, Leevers PS, Yayla P. Rapid crack propagation in pressurized plastic pipe. I: full scale and small scale RCP testing. Eng Fract Mech 1992;42:663–73.
[7] Yayla P, Leevers PS. Rapid crack propagation in pressurized plastic pipe. II: critical pressures for polyethylene pipes. Eng Fract Mech 1992;42:675–82.
[8] Han L-H, Deng Y-C, Liu C-D. The determination of JIC for polyethylene pipe using non-standard arc-shaped specimen. Int J Pressure Vessels Piping 1999;76:647–51.
[9] Leevers P. Impact and dynamic fracture of tough polymers by thermal decohesion in a Dugdale zone. Int J Fract 1995;73:109–27.
[10] García Brosa V, Bernal C, Frontini P. Calibration of fracture mechanics parameters and J–R curve determination in polyethylene side-grooved arc-shaped specimens. Eng Fract Mech 1999;62:231–48.
[11] Frassine R, Rink M, Pavan A. Discontinuous creep crack growth in polyethylene. Plastics, Rubber Compos, Process Appl 1996;25:1–5.
[12] Kenner VH, Popelar CH, Popelar SF. Proceedings of ICF7, Houston, USA, 1989. p. 2853/2859 (Part I) and p. 2861/2869 (Part II).
[13] ISO/DIS 17281 Standard. Ausgabe: 2001-2003, Plastics—determination of fracture toughness (G_{IC} and K_{IC}) standard for determining for plastics at moderately high loading rates (1 m/s).
[14] Kanninen M, Propelar C. Advanced fracture mechanics. 1985. p. 555 [chapter 4].
[15] Leevers PS, Morgan RE. Impact fracture of polyethylene: a non-linear-elastic thermal decohesion model. Eng Fract Mech 1995;52(6):999–1014.
[16] Pavan A, Williams JG. Development of a standard for determining K_{IC} and G_{IC} for plastics at high loading rates: the ISO/DIS 17281 standard for 1 m/s testing, limitations of test methods for plastics, ASTM STP 1369, 1999.
[17] Williams JG, Adams GC. The analysis of instrumented impact tests using a mass-spring model. Int J Fract 1987;33:209–22.
[18] Plati E, Williams JG. The determination of the fracture parameters for polymers in impact. Polym Eng Sci 1975;15:470–7.
[19] Williams JG, Cawood MJ. European group on fracture: K_c and G_c methods for polymers. Polym Testing 1975;9:15–26.
[20] Standard test method for plane-strain fracture toughness of metallic materials. ASTM E399-90-A9.
[21] MathCad 2001 Professional. MathSoft Inc.
[22] LUSAS Analyst Version 13.3, FEA Ltd, Forge House, 66 High Street, Kingston UponThames, Surrey, England.
[23] Pavan A, Draghi S. Further experimental analysis of the dynamic effects occuring in three-point bending fracture testing at moderately high loading rates (1 m/s) and their simulation using an ad hoc mass-spring-dashpot model, Les Diablerets, Switzerland, 13–15 September 1999. In: Williams JG, Pavan A, editors. Fracture of polymers, composites and adhesives. ESIS Publication 27.
[24] Williams JG. In: Fracture mechanics of polymers. Chichester: Ellis Horwood; 1984. p. 247.